Eur. Phys. J. B **51**, 363–371 (2006)
DOI: 10.1140/epjb/e2006-00241-7

THE EUROPEAN PHYSICAL JOURNAL B

Braid theory and Zipf-Mandelbrot relation used in microparticle dynamics

K. de Lange Kristiansen[1,2,a], G. Helgesen[2], and A.T. Skjeltorp[1,2]

[1] Department of Physics, University of Oslo, Blindern, 0316 Oslo, Norway
[2] Physics Department, Institute for Energy Technology, 2027 Kjeller, Norway

Received 16 November 2005 / Received in final form 30 March 2006
Published online 21 June 2006 – © EDP Sciences, Società Italiana di Fisica, Springer-Verlag 2006

Abstract. A study is presented of the dynamics of a few body system of microparticles by using rank-ordering statistics in order to gain insight in the magneto-rheological properties of ferrofluids. This dynamical system is made up of micrometer sized plastic spheres dispersed in a ferrofluid driven by external magnetic fields. The world lines of the microspheres are captured and the dynamical modes are described by mathematical braid theory. Rank-ordering statistics on these modes shows a wide power law region consistent with the *Zipf-Mandelbrot relation*. We have also performed numerical simulations of the experimental system which show results in agreement with the observations.

PACS. 05.45.-a Nonlinear dynamics and chaos – 83.10.Pp Particle dynamics – 02.10.Kn Knot theory – 75.75.+a Magnetic properties of nanostructures

1 Introduction

An understanding of the magneto-rheological (MR) properties of ferrofluids [1] is of general interest for both fundamental research [2], and industrial application. Ferrofluids change their viscous properties when subjected to an external magnetic field, which is exploited for e.g. damping systems in passenger vehicles and damping systems for protecting buildings and bridges from earthquakes and windstorms [3]. This so called magnetoviscous effect was first observed by McTague [4]. This effect can be explained by magnetic torques acting upon the ferromagnetic particles in the suspension [5]. In diluted ferrofluids rotary Brownian motion of non-interacting rigid dipoles experiences a rotational friction [6]. This has been shown to give an additional enhancement of the viscosity. The rotational viscosity is not well explained in semi-diluted ferrofluids in external oscillating or rotating fields. This is partly caused by the lack of understanding of the dynamical processes that take place. It has been proposed that the discrepancy between theoretical predictions and the experimental results are due to interactions among ferrofluid particles, formation and break-up of chains [7–9]. Some of these processes may be uncovered and clarified by studying similar systems of magnetically interacting particles with sizes in the optically visible micrometer range. One such system is created when micrometer sized plastic particles are dispersed in a ferrofluid. Then the magnetic voids create so-called magnetic holes [10]. As will be shown below this system exhibits complex formation and break-up of particle chains.

The magnetic holes system has proven to be a fruitful model for studying cooperative dynamical processes. Using microparticles of size >10 μm the thermal motion is negligible and the only forces which have to be taken into consideration are the viscous and magnetic forces. In this study braid theory will be used for describing the dynamical modes of the colloidal particles. The braid theory gives a compact description of entangled lines in three dimensional space, e.g. the spatiotemporal dynamics of particles moving in two dimensions [11,12], braided magnetic lines [13], and fluid flow dynamics [14,15]. For particle dynamics the idea is to transform the real trajectories of the particles in space-time to the corresponding symbolic sequence according to braid theory, see Figure 1. A symbol σ_i in our notation, denoted the braid generator, tells how two particles move relative to each other.

Dynamical systems may be described by simple laws, but give rise to richly intricate structures and complex behavior. Their dynamical modes may be distributed over a large energy range or other corresponding measurable quantities. In intermittent systems these modes have a broad distribution of frequencies. One way of making a systematic study of these modes is by ordering them after their occurrence frequencies. We let the mode which occur most often be ranked as number 1, the second most occurring mode be ranked number 2, and so forth to the

[a] *Current address*: Department of Chemical Engineering, 3357 Engineering II, University of California, Santa Barbara, CA 93106, USA; e-mail: kaidk@fys.uio.no

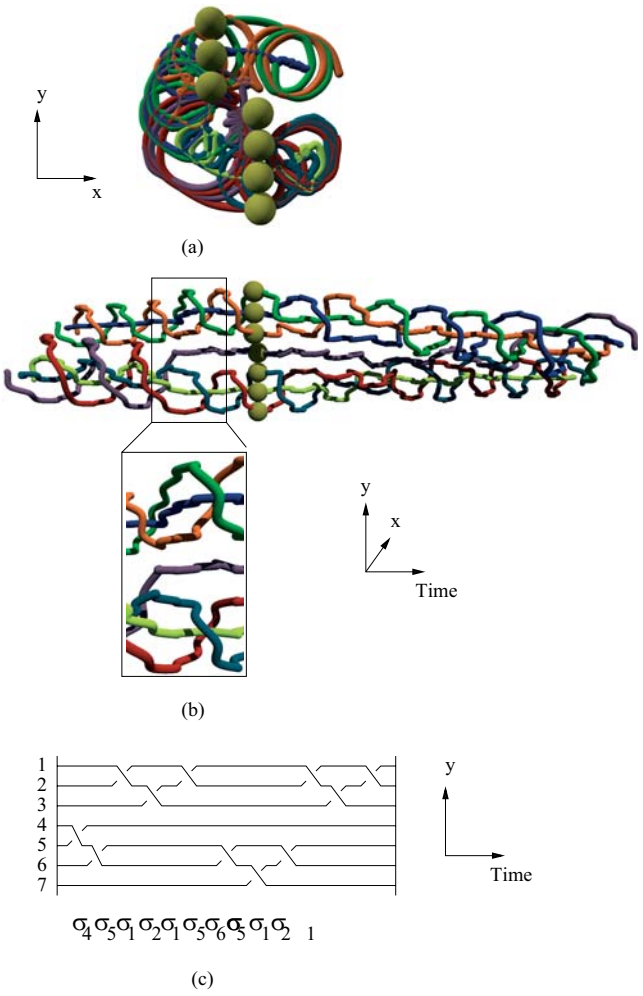

Fig. 1. Application of braid notation to particle dynamics. (a) The two-dimensional motion of 7 microspheres is extended to (b) three-dimensional space-time with the trace of each particle in time. (c) The strands are numbered from top to bottom relative to the y-axis. When two particles (i and $(i+1)$) exchange places relative to the y-axis the notation is σ_i for counterclockwise rotation and σ_i^{-1} for clockwise rotation. The motions of the 7 microspheres are taken from an experiment with seven spheres, $\epsilon = 0.67$, and $\omega = 0.23$.

least occurring mode which have the highest rank number. This rank-ordering statistics [16] takes care of both common and rare events at the same time and this procedure is useful for displaying the whole range of the mode distribution.

A remarkable feature found by rank-ordering statistics in many different systems is the Zipf relation. This relation has been found in a variety of applications, such as linguistics [17], energy distribution of earthquakes [18] and in analyzing the coding and non-coding regions of DNA sequences [19]. The original Zipf relation came into being in an empirical manner in linguistics. By analyzing the occurrence of words in large written texts G.K. Zipf proposed a simple power law $\phi(r) \sim r^{-\gamma}$ with $\gamma = 1$, where $\phi(r)$ is the frequency of occurrence of a word with rank r [17]. The origin of this relation has been connected to

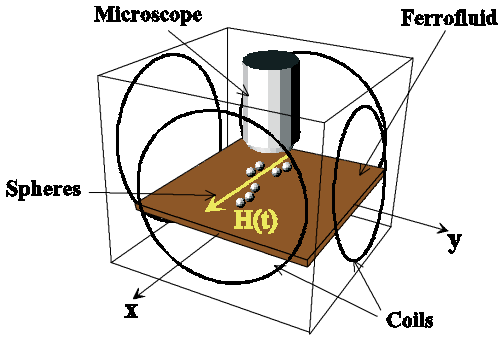

Fig. 2. The experimental set-up.

the hierarchical structures of languages [20], and gives the corrected Zipf-Mandelbrot relation [21]:

$$\phi(r) = \frac{A}{(r+\zeta)^{\gamma}}, \tag{1}$$

where A is a normalization constant and ζ is a parameter. In this work we report experiments and numerical simulations on a dynamical system, the magnetic holes system, which shows this Zipf-Mandelbrot relation.

The words in linguistics or the code of DNA sequences carry information. Dynamical systems, like the magnetic holes system, also generate information which is contained in the variety of the modes. This information can be quantified in terms of the Shannon entropy [22] together with its related redundancy.

The paper is organized as follows. In Section 2 we introduce the notion of magnetic holes and describe our experimental system. In Section 3 we present a simple model for this system, and Section 4 describes how we analyse the motion in terms of braid theory. The results from both experiments and numerical simulations are given in Section 5. Here we find that the rank-ordering statistics gives results according to the Zipf-Mandelbrot relation. In addition there are discussions on the temporal correlations and on the information content of the system in terms of Shannon entropy. A short summary of the results are given in Section 6. Finally, the Appendix gives a more detailed explanation of the elements of braid theory used in this work.

2 Experiment

The magnetic holes system is easily realized by dispersing uniformly sized polystyrene spheres [23] with diameter 50 μm in a ferrofluid [24] which is confined to a $\sim$100 μm thin layer, Figure 2. The ferrofluid consists of nm-sized magnetite particles dispersed in kerosene. In the magnetic holes system external magnetic fields induce a magnetic moment on the microparticles, where all moments have equal strength and direction. When the external magnetic field is rotating, the microparticles perform a collective motion. The rotational and translational diffusion of the particles is negligible for the present system.

The external planar, elliptically polarized field $\boldsymbol{H}(t)$ is produced by two pairs of coils mounted perpendicular to

each other carrying AC current with a phase difference of $\pi/2$. The amplitude components H_x and H_y are varied by adjusting the maximum current through a pair of coils. The field anisotropy parameter is defined as $\epsilon = H_y/H_x$. For the experiments presented in this study we use $H_x =$ 27 Oe.

In a slowly rotating external magnetic field, the microspheres try to line up in chains parallel with the field. Due to viscous forces there will be a phase lag between the direction of the magnetic field and the chains of microspheres. The chains will furthermore break up in smaller subchains and perform a half rotation before aligning again. For example, a chain of 7 microspheres was observed to split into groups of $3+2+2$ or $3+3+1$. A circularly polarized magnetic field gives a highly periodic motion where the chain divides into groups with close to equal number of spheres [25]. In an elliptically polarized magnetic field, on the other hand, the division into subchains is so irregular that we get an apparently disordered behavior. In the frequency range studied here, the microspheres are nearly co-linear every half period of the external field. This suggests that in order to investigate the main dynamics we can focus on what happens along a fixed direction.

3 The simulation model

The microspheres are diamagnetic and will modify the magnetic field in the ferrofluid by introducing nonmagnetic voids, called magnetic holes [10]. Due to the demagnetization of the void, the magnetic hole will carry an apparent magnetic moment $\boldsymbol{m}(t)$, located in the center of the microsphere and pointing in opposite direction of the magnetic field $\boldsymbol{H}(t)$. Its strength is proportional to the volume V of displaced ferrofluid, the ferrofluid's effective susceptibility χ_{eff} and the field $\boldsymbol{H}(t)$,

$$\boldsymbol{m}(t) = -\chi_{eff} V \boldsymbol{H}(t), \tag{2}$$

where $\chi_{eff} = \frac{3\chi}{3+2\chi}$ includes the demagnetization factor of a sphere, and χ is the bulk magnetic susceptibility of the ferrofluid.

These magnetic holes interact via dipole interactions, and the interaction energy U for a collection of n magnetic holes is given by:

$$U(\boldsymbol{r}_1, ..., \boldsymbol{r}_n, t) = \begin{cases} \sum_{i>j}^{n} \frac{m^2(t)}{r_{ij}^3} - \frac{3\cdot[\boldsymbol{m}(t)\cdot\boldsymbol{r}_{ij}]^2}{r_{ij}^5}, & r_{ij} > d \\ \infty, & r_{ij} < d \end{cases} \tag{3}$$

where $\boldsymbol{r}_{ij} = \boldsymbol{r}_i - \boldsymbol{r}_j$ is the vector joining the centers of the magnetic holes and d is the diameter of a microsphere. The magnetic force on particle i is then:

$$\boldsymbol{F}_i^M = \frac{\partial U(\boldsymbol{r}_1, ..., \boldsymbol{r}_n, t)}{\partial \boldsymbol{r}_i}. \tag{4}$$

The viscous force on a microsphere is to first order given by Stokes' law:

$$\boldsymbol{F}^{Stokes} = 3\pi\eta d\boldsymbol{v}, \tag{5}$$

where η is the viscosity of the ferrofluid and $\boldsymbol{v}$ the velocity of the sphere. Since the diameter of the microspheres and their velocities are relatively small, the Reynolds number, $Re = \rho v d/\eta \ll 1$, where ρ is the ferrofluid density. The system is therefore overdamped and we may neglect the inertia forces [26]. By assuming equilibrium between the magnetic and viscous forces,

$$\sum \boldsymbol{F} = \boldsymbol{F}^M + \boldsymbol{F}^{Stokes} = 0, \tag{6}$$

we can easily transform the equation of motion into a numerically solvable form [11].

The angular velocity ω_H of the external field is normalized by the critical angular velocity ω_c for stable rotation of two microspheres with a circularly polarized magnetic field [26]:

$$\omega = \omega_H/\omega_c, \tag{7}$$

where $\omega_H = 2\pi f$ and f is the frequency of the rotating magnetic field. At ω_c a chain of two microspheres starts to show phase-slips relative to the magnetic field, and in our experiments this upper angular velocity for stable rotation is $\omega_c = 2\pi \cdot 0.62\ \mathrm{s}^{-1}$.

4 Data analysis and braid theory

The motion of the n interacting magnetic holes is observed with a light microscope and the images are acquired with an attached video camera and recorded and digitized on a workstation. Typically 5 images per second are grabbed and analyzed by the workstation. A computer program is used to map the positions of the microspheres in the (x, y)-plane in real time, Figure 1a. Our next step in the analysis is to include the time, in order to obtain a space-time diagram (x, y, t), thus, creating the world-lines of the microspheres. In this way we essentially "freeze" the dynamics of the microspheres at all times, Figure 1b. The geometrical braid, Figure 1c, will appear when projecting the space-time trajectories onto one of the spatial axis [25].

The braid generators, σ_i, are read out from the geometrical braid and the resulting sequence of braid generators gives the braidword. The set of all braids with n-strands is the Artin braid group B_n, containing every possible rotations of n magnetic holes. The braidwords found in experiments may not be topologically unique due to continuous deformations [27]. The challenge is to find a scheme to determine whether two braidwords are equivalent and thereby describe the same dynamics. This so called *word problem* has been solved for B_n [28]. A refinement of this solution, the *Garside algorithm* which is used in this analysis, is found in reference [29], see Appendix A.

After running through the Garside algorithm the braidword are represented by an ordered set of *positive permutation braids*. The positive permutation braids are small parts of the braidword and belong to a subset of B_n with two additional criteria: 1) the strands of space-time diagram have only overcrossings; and 2) two strands can cross each other only once.

Table 1. The experimental parameters, n, ϵ, and ω, and the values for the best fit of the data set to equation (1) for four experiments.

Exp.	n	ϵ	ω	A	ζ	γ
1	7	0.67	0.23	3.2 ± 0.1	5.3 ± 1.0	1.8 ± 0.1
2	7	0.83	0.44	0.68 ± 0.10	1.7 ± 0.5	1.4 ± 0.1
3	11	0.64	0.22	0.12 ± 0.05	1.2 ± 0.2	0.98 ± 0.10
4	20	0.64	0.15	0.0091 ± 0.0005	1.5 ± 0.2	0.80 ± 0.08

The so called *factorial coordinate* method [29] is a convenient and unique way of labelling the different positive permutation braids. The algorithm for this method is given by the expression:

$$g(\tau) = 1 + g_1(\tau)1! + ... + g_{n-1}(\tau)(n-1)! \quad \text{with} \quad 0 \leq g_i(\tau) \leq i. \tag{8}$$

The factorial coordinate $g_i(\tau)$ counts the number of crossings of string $i+1$ with lower number strings within the positive permutation braid $g(\tau)$ after a time τ. One permutation braid typically corresponds to one half period of the rotating magnetic field.

The system is driven by an external rotating magnetic field so the system of magnetic holes as a whole will rotate, or in braid theory language obtain a positive half twist. This effect is particularly important for a low number of spheres ($n < 10$) and low field anisotropy ($\epsilon > 0.7$). Since the motion of the microspheres is captured in the laboratory frame the braid includes these unwanted half twists. The Garside algorithm will extract these positive half twists. The finale positive permutation braids contain all the essential information about the dynamics, and are taken as a measure of the physical modes.

5 Results and discussion

In this study we focus mainly on experiments with seven microspheres that have the anisotropy parameter ϵ between 0.58 and 0.85, and the angular frequency ω in the range $0.23 < \omega < 0.45$. In these parameter ranges intermittent behavior is observed. This behavior generates many different modes with different frequency of occurrence, and is easily studied with the rank-ordering statistics. Outside these parameter ranges more regular behavior is observed. For experiments with a higher number of spheres n, we have studied what happens around $\epsilon = 0.64$. The experiments were run from 4 to 13 h. In this work we present four different experiments with different n, ϵ, and ω values. The experimental values are summarized in Table 1.

The motion is grabbed and analyzed by a computer in real time. In this analyzing process the coordinates of each sphere is found, Figure 1a and 1b, and also the braid generators, Figure 1c. Two factors are striking when observing the motion of the spheres:

1. the spheres start out in a line and get almost aligned after one half period of the external rotating field. During this half period the line of spheres breaks up into smaller units before realigning;
2. some typical and stable modes occur frequently over some time. Then the motion is changing via a cascade of different and rarer modes for some time before reaching a stable mode again. This resembles intermittent behavior.

The first factor emphasizes that the time span for a dynamical mode is around one half period of the external rotating magnetic field. The second factor suggests that the system behaves like a scaling tree, similar to the lexicographic tree described by Mandelbrot for word frequencies in linguistics [30]. He used this scaling tree to derive the Zipf-Mandelbrot relation. A similar approach can be used to derive this relation for the system under study here [31].

5.1 Rank-ordering statistics

A small part of experiment No. 1 with $\epsilon = 0.67$ and $\omega = 0.23$ is displayed in Figure 1. Seven spheres trace out their world lines and are projected into a braidword. The different dynamical modes of this experiment are measured and displayed in terms of their corresponding g-values in Figure 3. We obtain 365 different dynamical modes in the experiment, while for the numerical simulations with same duration we obtain 392 different modes. A significant feature is that a small set of modes appears frequently and is interrupted by rarer modes. Small variations in the system parameters might lead to large changes in the braidword and the g-values. This can be seen in the differences between the experiment, Figure 3a, and the simulation, Figure 3b, which have nominally equal parameter values. However, these minor changes do not change the overall statistical properties of the dynamics.

We then apply rank-ordering statistics to these braid permutations. In rank-ordering statistics we count all the different modes and rank them afterwards. The rank r of a mode is defined such that the most frequently occurring mode gets the rank $r = 1$, the next most frequently used mode gets rank 2, etc. The frequency of occurrence $\phi(r)$ is normalized: $\sum_{r=1}^{N} \phi(r) = 1$, where N is the total number of different modes. Including all types of positive permutation braids for n strands, $N = n!$. For the case of seven microspheres we have $N = 5040$ possible modes.

The rank-ordering analysis of the positive permutation braids is shown in a double logarithmic plot in Figure 4. The data may be fitted to a straight line with a slope -1.6 ± 0.1 for $r > 5$. However, a nonlinear fit on

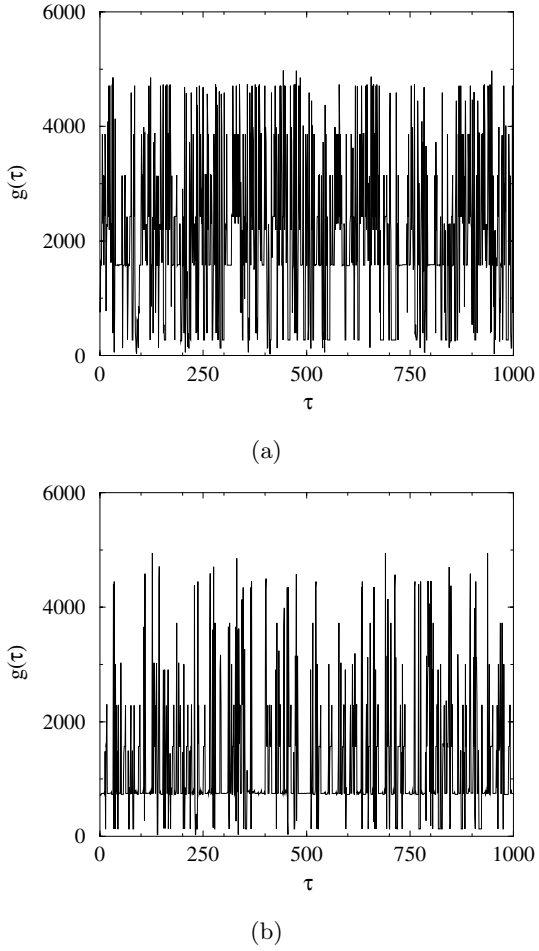

Fig. 3. The dynamics of 7 microspheres in an external rotating magnetic field is displayed in terms of the factorial coordinates of the positive permutation braids $g(\tau)$ as a function of the time τ for (a) experiment No. 1 and (b) its corresponding simulation. The most frequent modes (e.g. groups of $1+3+3$ spheres, $g = 1575$ (experiment) or $3+2+2$ spheres, $g = 750$ (simulation)) reflect the symmetry in the system as opposed to rarely occurring modes (e.g. $1+1+1+3+1$ spheres, $g = 265$).

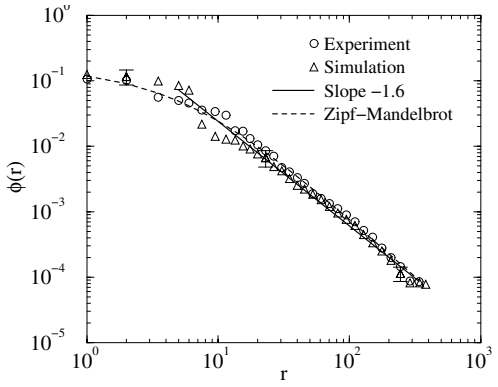

Fig. 4. The frequency of occurrence of braid permutations $\phi(r)$ versus its rank r found in the dynamics of 7 microspheres, experiment No. 1 with $\epsilon = 0.67$ and $\omega = 0.23$. Both data sets fit well to the Zipf-Mandelbrot relation, shown as a dashed line. Typical values of the error bars are shown for three points.

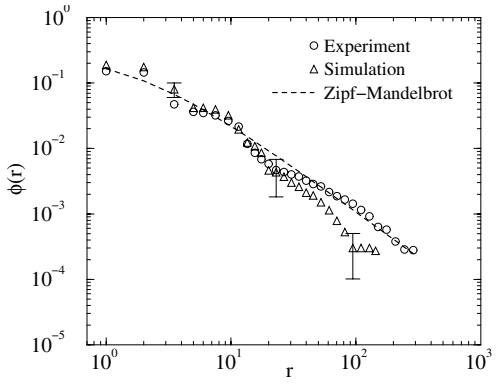

Fig. 5. The frequency of occurrence of braid permutations $\phi(r)$ versus its rank r found in the dynamics of 7 microspheres with $\epsilon = 0.83$ and $\omega = 0.44$, experiment No. 2. Typical values of the error bars are shown for three points.

the whole r-range to the Zipf-Mandelbrot relation, equation (1), gives a better fit with parameters $A = 3.2 \pm 0.2$, $\zeta = 5.3 \pm 1.0$ and $\gamma = 1.8 \pm 0.1$ for both experiment and simulation. A simulation with four times longer duration gives 448 different types of dynamical modes, however the fit gives the same parameter values. This is a common feature for all our results presented here. A large subgroup of the data displays the same form of Zipf-Mandelbrot relation. The only difference is that some of the modes occurring a few times are not present.

Similar behavior to that discussed above is also observed for experiments with other values of ϵ and ω , and the exponent γ is found to be between 1.1 and 1.9, as first reported in reference [32]. The experiment No. 2 is an example with $\epsilon = 0.83$ and $\omega = 0.68$. The rank-ordering analysis of this experiment gives a Zipf-Mandelbrot relation between $\phi(r)$ and r, Figure 5, with exponent $\gamma = 1.4$.

The value of the exponent γ found in the simulations sometimes shows slightly higher value than that obtained from the corresponding experiment. This difference between experiment and simulation may be due to higher order effects neglected in the simulation, such as hydrodynamic interaction between microspheres and hydrodynamic and magnetic interaction due to confinement of the ferrofluid by the walls. In dispersed systems, such as colloidal suspensions, complicated flow behaviors occur even at low Reynolds numbers. Despite its long-recognized ubiquity, hydrodynamic coupling in colloidal suspensions is not completely understood [33].

The Zipf-Mandelbrot relation is observed in systems with higher number of spheres as well. Figures 6 and 7 are examples of 11 and 20 spheres, respectively. For both cases we used $\epsilon = 0.64$. The results are summarized in Table 1. When increasing the number of spheres the number of possible modes increases rapidly. For eleven spheres there exist $11! \simeq 4.0 \times 10^7$ possible modes, while we obtained only 2200 modes in experiment No. 3. Twenty spheres have $20! \simeq 2.4 \times 10^{18}$ possible modes and the simulation

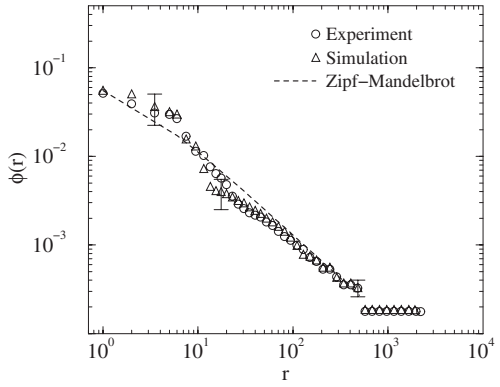

Fig. 6. The frequency of occurrence of braid permutations $\phi(r)$ versus its rank r found in the dynamics of 11 microspheres with $\epsilon = 0.64$ and $\omega = 0.22$, experiment No. 3. Typical values of the error bars are shown for three points.

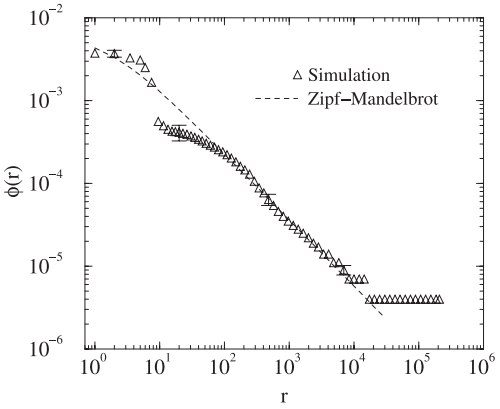

Fig. 7. The frequency of occurrence of braid permutations $\phi(r)$ versus its rank r found in the dynamics of 20 microspheres with $\epsilon = 0.64$ and $\omega = 0.15$, simulation No. 4. Typical values of the error bars are shown for four points.

gave only 30 000 modes. To observe a behavior obeying the Zipf-Mandelbrot relation for systems with $n \geq 10$, we need experiments over a longer time span in order to get good statistics. The exponents fitted to the experiment and simulation are both below 1 and significantly lower than for the seven spheres case.

5.2 Temporal correlation

To get a measure of the temporal correlation of the positive permutation braids in the system we calculate the mode-mode correlation between modes of rank r and r':

$$C_{r,r'}(t) = \langle \delta_{r,r(g(\tau))} \delta_{r',r(g(\tau+t))} \rangle, \tag{9}$$

where brackets indicate averaging over all times τ, $r(g(\tau))$ means the rank corresponding to mode $g(\tau)$ and t is a time interval measured in units of one permutation braid. The exact numerical value of the $g(\tau)$'s are of little interest here since that is only a way of systematic labelling. The

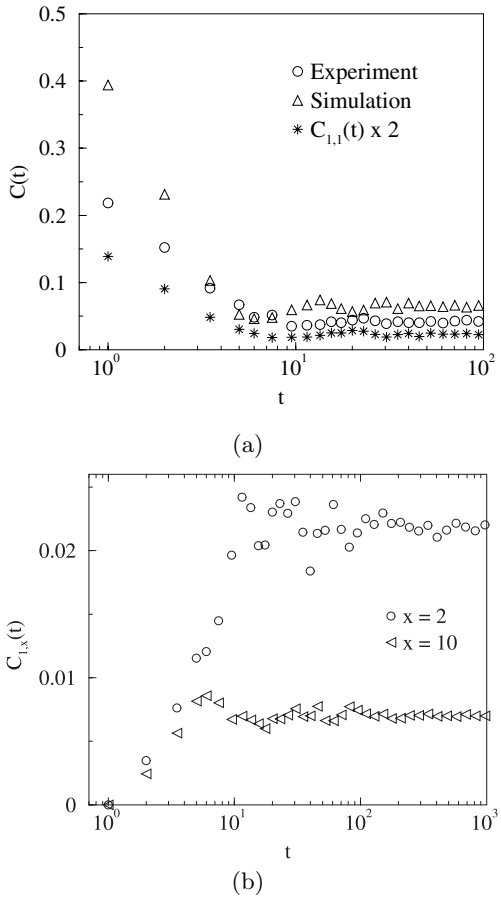

Fig. 8. (a) The time correlation of the braid permutations $C(t)$ displayed on a semi-log plot. The time t is measured in number of permutation braids in the braidword. The correlation of the mode with rank $r = 1$, $C_{1,1}(t)$ (scaled up by a factor 2) from the experimental data of experiment No. 1, is also shown. (b) The correlations between the most frequently occurring mode, $r = 1$, and the modes with rank 2 and 10, respectively, taken from experiment No. 1.

time correlation $C(t)$ is defined as:

$$C(t) = \sum_{r=r'=1}^{N} C_{r,r'}(t). \tag{10}$$

When no correlations between the permutation braids are left in the system, we expect a crossover to a plateau at level K in $C(t)$:

$$K = \sum_{r=1}^{N} \phi(r)\phi(r). \tag{11}$$

The correlation between the modes in experiment no. 1 is short ranged and decays logarithmically for $1 < t < 6$ as shown in Figure 8, and thereafter shows a plateau. Similar decay is found for the other experiments. The correlation of modes with low r-value dominates $C(t)$, as e.g. $C_{1,1}(t)$ for $r = 1$, reflecting that dominating modes occur in sequences. For 7 microspheres the plateau after the cutoff

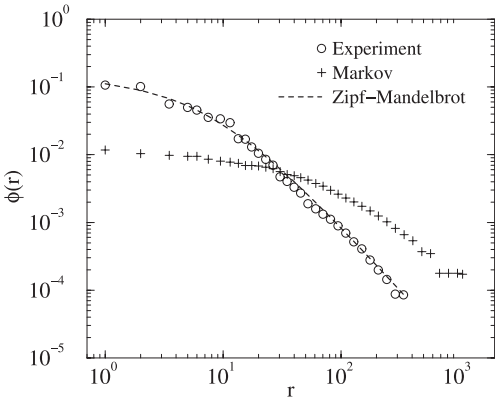

Fig. 9. The experiment from Fig. 4 together with a Markov process with transition matrix based on this experiment.

can be calculated from equation 1 using the fitted parameter values, $K = 0.043$, in good agreement with Figure 8a. We have also calculated the correlations $C_{1,2}(t)$ and $C_{1,10}(t)$ between the modes with rank 1 and 2, and 1 and 10, respectively, as shown in Figure 8b. The $C_{1,x}(t)$ rises to a constant level depending on the rank x. A characteristic feature is that a dominating mode tends to be interrupted by another mode within the decay time of $C(t)$.

The correlation up to $t = 6$ is the result of clustering of the modes. If we randomize the order in the sequence of modes, these correlations disappear and only a plateau is left, as expected.

Markov processes have been used to explore Zipf relation in linguistics [34]. We will use the same procedure to investigate the effect of correlations of the braid generators. A one step Markov chain is generated using the conditional probability $P(\sigma_i|\sigma_j)$ of achieving σ_i given σ_j. The $P(\sigma_i|\sigma_j)$ is found from the actual experiment. For a completely random sequence of braid generators, $P(\sigma_i|\sigma_j) = c$ for all i and j, which gives a flat Zipf-Mandelbrot plot. With a correlation time shorter than that of the current experiment the Markov process will give a more random sequence of braid generators. As seen above the experiment has correlation length of $t \sim 5$. This means that the correlation length is about 30 braid generators, as one time step contains one mode and a typical frequent mode was found to be about 6 braid generators. Thus we expect a much broader distribution of the modes when using the Markov process compared to the experimental results. This is indeed what we see in Figure 9, where the parameters are: $A = 4.6$, $\zeta = 57$, and $\gamma = 1.5$.

5.3 Information and redundancy

The braidword can be viewed as a discrete message built out of smaller units, which are the positive permutation braids. The statistics of these units is dominated by those which transmit the greatest amount of information, and is quantified in terms of Shannon entropy H [35]:

$$H = -\sum_{k=1}^{N} \phi_k \log_2 \phi_k, \tag{12}$$

where the unit is bits/(mode).

H is a measure of the rate of information which is produced. For equally probable situations, $\phi_k = 1/N!$, and the entropy is maximum, i.e. no prediction of the next entry. For the case of seven spheres, $H_{max} = \log_2 5040 = 12.30$. The redundancy R is then defined as [22]:

$$R = 1 - \frac{H}{H_{max}}. \tag{13}$$

Table 2. The Shannon entropy H and the redundancy R for the three experiments in Table 1, where H is calculated using the values for the best fit, Table 1.

Exp.	N	H	R
1	7	5.43 ± 0.10	0.56 ± 0.01
2	7	5.96 ± 0.10	0.52 ± 0.01
3	11	6.72 ± 0.10	0.73 ± 0.01
4	20	4.5 ± 1.0	0.93 ± 0.02

Table 2 summarizes the entropy and redundancy for each experiment. The relative high redundancy in these cases reflects the fact that there exists many more modes than those found in the experiments. As the number of spheres increases, the number of possible positive permutation braids increases as $N!$. For the experiments in this work the fraction of observed modes compared to the possible number of modes decreases as the number of spheres increases. In addition, sequences of the motion repeat from time to time, thereby increasing the redundancy.

6 Conclusion

Braid theory has been used to study the collective dynamical processes, or modes, of magnetically interacting particles in a rotating magnetic field. An n-stranded space-time braid represented the motions of non-magnetic microspheres in a thin ferrofluid layer. We extracted the positive permutation braids and used these as a measure of the collective modes in the system. The distribution of these dynamical modes was analyzed using rank-ordering statistics, and it was found to show a hierarchical structure of the Zipf-Mandelbrot type. For seven spheres the exponent γ was between 1.1 and 1.9 for both experiments and numerical simulations. Similar distributions of the dynamical modes were found for systems containing a higher number of microspheres as well. But for these cases the exponent γ could also have lower values than 1.1. As the number of spheres increased, the number of possible modes increased drastically. The temporal correlation of the modes decayed logarithmically, as the result of clustering of the most frequent modes. The clustering was also one of the reasons for the relative high redundancy. This

showed that many of the possible modes never occurred in the experiments.

The magneto-rheology of ferrofluids in oscillating or rotating fields has been extremely difficult to model by current theories. This may be due to the complexity of the chain formation and break-up in even such relatively small particle clusters as studied here. The wide spectrum of relaxation times and other effects, like shear thinning, which have been found in these fluids, may have their origins in the distributions of dynamical modes and chain lengths. This is similar to what has been found in the system presented here.

KdLK is grateful to the Research Council of Norway for financial support (grant NFR 142902/432).

Appendix: The garside algorithm

The aim of this algorithm is to start from a braidword P and transform it to a right canonical form $P = P'(\Delta_n)^q$ [28,29]. The P' is a sequence of positive permutation braids: P_1, P_2,..., P_N, and q is the number of positive half twists Δ_n. The positive half twist can be defined inductively in terms of the braid generators: $\Delta_n = \Delta_{n-1}\sigma_{n-1}\sigma_{n-2}...\sigma_1$ starting with $\Delta_2 = \sigma_1$. The n indicates the number of strings. Normally we omit n, i.e. $\Delta \equiv \Delta_n$, when it does not lead to any confusion. The right-canonical form implies that any other braid Q topologically equal to P will give the same exponent q and sequence of positive permutation braids P', with the twists on the right hand side of P'. The P' is now the simplest sequence of positive permutation braids, and it is irreducible and unique.

In order to work with positive permutation braids each negative braid generator in the braidword must be replaced. This can be done by rewriting every σ_i^{-1} as $D\Delta^{-1}$ where D is a positive braid word. Thereafter all the Δ's is moved to the right by using the commutativity of Δ with all other braid structures B, i.e. $\Delta \cdot B = \tau(B)\Delta$, where $\tau(B)$ is an automorphism operating on the braid B. Geometrically it is equivalent to turning the braid upside down and is defined as $\tau(\sigma_i) = \sigma_{n-i}$. The next step is to divide the positive braid into a product of positive permutation braids. In this algorithm we start reading the braid from left to right and take the longest initial subword as the first permutation. A new permutation braid is started when any pair of the strings is about to cross for the second time. This division is continued until the end of the braid word is reached.

The algorithm prescribes to run through P' from left to right and checks adjacent pairs of permutation braids. If any crossing of pair of adjacent strings occurs in the left permutation braid and not in the right, this crossing is moved to the right permutation braid. This yields two different permutation braids. Each time a positive half twist is found in the sequence it is moved to the right end of the braid where it contributes to the power of Δ^q with $+1$. The algorithm goes on until no more moves or operations

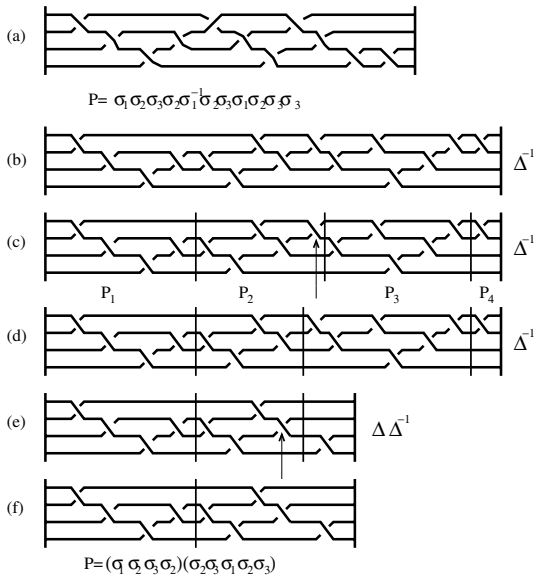

Fig. A.1. A sequence of moves leading to the right canonical form of a braid as described in the text.

can be done and the right canonical form of the braid is found. The right canonical form gives the minimum number of positive permutation braids that the braid can be divided into.

Let us apply this algorithm to the example with four strings shown in Figure A.1, which describes a braid with the word $P = \sigma_1\sigma_2\sigma_3\sigma_2\sigma_1^{-1}\sigma_2\sigma_3\sigma_1\sigma_2\sigma_3\sigma_3$. The first step is to replace any braid generators with negative powers. The generator σ_1^{-1} in (a) is replaced by $\sigma_2\sigma_3\sigma_1\sigma_2\sigma_1\Delta^{-1}$ and the negative half twist is moved to the right end of the sequence, resulting in (b). Working through the braid in (b) from left to right we partition it into permutation braids by continuing until a pair of strings are about to cross for the second time and then start a new permutation braid, shown in (c). Then we start the algorithm to check adjacent pairs of permutation braids if any adjacent pairs of strings cross in the left, but not in the right permutation braid. Starting from the left end of the sequence, the first such crossing is found in the second permutation P_2 in (c) as indicated by an arrow. This crossing is moved to the third permutation P_3 which yields the two altered permutation braids P_2 and P_3 shown in (d). By this alternation, $P_3 = \Delta$, which has to be shifted to the right end of the braid. The permutation braid P_4 undergoes the operation $\Delta \cdot B = \tau(B)\Delta$. In this case $B = \sigma_1$, which gives $\tau(\sigma_1) = \sigma_3$. This gives the braid sequence shown in (e). Here, every braid generators in P_2 can in fact be shifted to P_3. Since P_2 then become the *identity braid*, i.e. a braid not containing any braid generator, it does not contribute to the braid and can therefore be discarded. At last the Δ at the end is cancelling out by the Δ^{-1}. The resulting braid in (f) is the right canonical form of P consisting of two permutation braids and $q = 0$, i.e. $P = (\sigma_1\sigma_2\sigma_3\sigma_2)(\sigma_2\sigma_3\sigma_1\sigma_2\sigma_3)$.

References

1. R.E. Rosensweig, *Ferrohydrodynamics* (Cambridge University Press, New York, 1985)
2. *Magnetic fluids and application handbook*, edited by B. Berkovski, V. Bashtovoy (Begel House Inc., New York, 1996)
3. K. Wollny, J. Läuger, S. Huck, Appl. Rheol. **12**, 25 (2002)
4. J.P. McTague, J. Chem. Phys. **51**, 133 (1969)
5. J. Embs, H.W. Müller, C. Wagner, K. Knorr, M. Lücke, Phys. Rev. E **61**, R2196 (2000)
6. M.I. Shliomis, Soviet Phys. JETP **34**, 1291 (1972).
7. S. Odenbach, H. Störk, J. Magn. Magn. Mater. **183**, 188 (1998)
8. F. Gazeau, C. Baravian, J.-C. Bacri, R. Perzynski, M.I. Shliomis, Phys. Rev. E **56** 614 (1997)
9. A. Zeuner, R. Richter, I. Rehberg, Phys. Rev. E **58** 6287 (1998)
10. A.T. Skjeltorp, Phys. Rev. Lett. **51**, 2306 (1983)
11. P. Pieranski, S. Clausen, G. Helgesen, A.T. Skjeltorp, Phys. Rev. Lett. **77**, 1620 (1996)
12. C. Moore, Phys. Rev. Lett. **70**, 3675 (1993)
13. M.A. Berger, Phys. Rev. Lett. **70**, 705 (1993)
14. P. L. Boyland, H. Aref, M.A. Stremler, J. Fluid Mech. **403**, 277 (2000)
15. *An introduction to the Geometry and Topology of Fluid Flows*, edited by R.L. Ricca (NATO ASI Series II, Kluwer, 2001), Vol. 47
16. E.J. Gumbel, *Statistics of Extremes* (Columbia University Press, New York, 1958)
17. G.K. Zipf, *Human Behavior and The Principle of Least Effort* (Addison-Wesley Press, Massachusetts, 1949)
18. D. Sornette, L. Knopoff, Y.Y. Kagan, C. Vanneste, J. Geophys. Res. **101**, 13883 (1996)
19. R.N. Mantegna, S.V. Buldyrev, A.L. Goldberger, S. Havlin, C.-K. Peng, M. Simons, H.E. Stanley, Phys. Rev. Lett. **73**, 3169 (1994)
20. B. Mandelbrot, Word **10**, 1 (1954)
21. B.B. Mandelbrot, *The Fractal Geometry of Nature* (W.H. Freeman, New York, 1982)
22. C.E. Shannon, Bell Syst. Tech. **27**, 379 (1948)
23. J. Ugelstad, P.C. Mørk, K. Herder Kaggerud, T. Ellingsen, A. Berge, Adv. Colloid Int. Sci. **13**, 101 (1980)
24. Type EMG 909 from Ferrofluidics GmbH, Hohes Gestade 14, 72622 Nürtingen, Germany, with susceptibility $\chi = 0.8$, saturation magnetization $M_s = 20$ mT, viscosity $\eta = 6 \times 10^{-3}$ N s m^{-2}, and density $\rho = 1020$ kg m^{-3}.
25. S. Clausen, G. Helgesen, A.T. Skjeltorp, Int. J. Bifurcation and Chaos **8**, 1383 (1998)
26. G. Helgesen, P. Pieranski, A.T. Skjeltorp, Phys. Rev. A **42**, 7271 (1990)
27. C.C. Adams, *The Knot Book* (W.H. Freeman and Company, 1994)
28. F.A. Garside, Quart. J. Math. **20**, 235 (1967)
29. E.A. Elrifai, H.R. Morton, Quart. J. Math. **45**, 479 (1994)
30. B.B. Mandelbrot, in *Proceedings of symposia in applied mathematics vol. XII*, edited by R. Jakobson (New York: American Mathematical Society, 1961)
31. K.D.L. Kristiansen, Ph.D. thesis, University of Oslo, 2005
32. K.D.L. Kristiansen, G. Helgesen, A.T. Skjeltorp, Physica A **335**, 413 (2004)
33. E.R. Dufresne, T.M. Squires, M.P. Brenner, D.G. Grier, Phys. Rev. Lett. **85**, 3317 (2000)
34. I. Kanter, D.A. Kessler, Phys. Rev. Lett. **74**, 4559 (1995)
35. C.E. Shannon, Bell Syst. Tech. **30**, 50 (1950)